Garel, J.-R., & Baldwin, R. L. (1973) *Proc. Natl. Acad. Sci. U.S.A. 70*, 3347–3351.

Goldenberg, D. P., & Creighton, T. E. (1985) *Biopolymers 24*, 167–182.

Grathwohl, C., & Wuthrich, K. (1981) *Biopolymers 20*, 2623–2633.

Harrison, S. C., & Durbin, R. (1985) *Proc. Natl. Acad. Sci. U.S.A. 82*, 4028–4030.

Hawkes, R., Grutter, M. G., & Schellman, J. A. (1984) *J. Mol. Biol. 175*, 195–212.

Hermans, J., & Scheraga, H. (1961) *J. Am. Chem. Soc. 83*, 3283–3292.

Ikai, A., & Tanford, C. (1973) *J. Mol. Biol. 73*, 145–163.

Ikai, A., Fish, W. W., & Tanford, C. (1973) *J. Mol. Biol. 73*, 165–184.

Jaenicke, R. (1988) *Prog. Biophys. Mol. Biol. 49*, 117–237.

Kim, P. S., & Baldwin, R. L. (1982) *Annu. Rev. Biochem. 51*, 459–489.

Laidler, K. J. (1950) in *Chemical Kinetics*, Chapter 3, McGraw-Hill, New York.

Matthews, C. R., & Hurle, M. R. (1987) *BioEssays 6*, 254–257.

Northrup, S. H., Pear, M. R., Lee, C.-Y., McCammon, J. A., & Karplus, M. (1982) *Proc. Natl. Acad. Sci. U.S.A. 79*, 4035–4039.

Pace, N. C., & Tanford, C. (1968) *Biochemistry 7*, 198–207.

Pohl, F. M. (1968) *Eur. J. Biochem. 7*, 146–152.

Privalov, P. L. (1979) *Adv. Protein Chem. 33*, 167–241.

Ptitsyn, O. B. (1987) *J. Protein Chem. 6*, 273–293.

Schellman, J. A. (1978) *Biopolymers 17*, 1305–1322.

Segawa, S.-I., & Sugihara, M. (1984) *Biopolymers 23*, 2473–2488.

Sturtevant, J. M. (1977) *Proc. Natl. Acad. Sci. U.S.A. 74*, 2236–2240.

Takagi, T., & Tanford, C. (1968) *Fed. Proc., Fed. Am. Soc. Exp. Biol. 27*, 338.

Tanford, C. (1961) in *Physical Chemistry of Macromolecules*, Chapter 8, Wiley, New York.

Tanford, C. (1968) *Adv. Protein Chem. 23*, 121–282.

Utiyama, H., & Baldwin, R. L. (1986) *Methods Enzymol. 131*, 51–70.

Weaver, L. H., & Matthews, B. W. (1987) *J. Mol. Biol. 193*, 189–199.

Wyman, J. (1964) *Adv. Protein Chem. 19*, 223–286.

NMR Studies of the Influence of Dodecyl Sulfate on the Amide Hydrogen Exchange Kinetics of a Micelle-Solubilized Hydrophobic Tripeptide[†]

Joe D. J. O'Neil and Brian D. Sykes*

MRC Group in Protein Structure and Function, Department of Biochemistry, University of Alberta, Edmonton, Alberta T6G 2H7, Canada

Received August 1, 1988

ABSTRACT: Backbone amide hydrogen exchange measurements are an important source of information about the internal dynamics of proteins. Before such measurements can be interpreted unambiguously, contributions to hydrogen exchange rates from the chemical and physical environment of the amides must be taken into account. Membrane proteins are often solubilized in detergents, yet there have not been any systematic investigations of the possible effects detergents may have on the amide hydrogen exchange rates of proteins. To address this question, we have measured individual backbone and carboxyl-terminal amide exchange rates for the amphipathic tripeptide Leu-Val-Ile-amide dissolved in water and dodecyl sulfate micelles. ^{1}H NMR spectroscopy was used to measure exchange using the direct exchange-out into D_2O technique at 5 °C and using an indirect steady-state saturation-transfer technique at 25 °C. The broadening effect of micelle-incorporated spin-labeled fatty acid (12-doxylstearate) on the ^{1}H NMR spectra of both the detergent and the peptide resonances was used to demonstrate that the tripeptide is intimately associated with the micelle. The resonance from formate ion, which is excluded from the micelle, was unperturbed by the spin label. The detergent did not retard the exchange rates of either the primary (terminal) or secondary (backbone) amides of the tripeptide. This suggests that the micelle/peptide interaction does not restrict access of charged catalysts and water to these amides and shows that the peptide amides are not hydrogen bonded. However, the pH for the exchange minima of these amides in detergent was increased between 1.2 and 1.7 units compared to exchange in water. This is due to the electrostatic effect of the negative charge on the sulfate groups that concentrate protons in their vicinity, effectively lowering the pH in the microenvironment of the amides. These experiments help to explain the elevated pH_{min} observed for backbone amides in the sodium dodecyl sulfate solubilized M13 coat protein [O'Neil, J. D. J., & Sykes, B. D. (1988) *Biochemistry 27*, 2753–2762].

$\mathbf{C}$haracterizing the dynamic aspects of protein structure will undoubtedly contribute to a better understanding of the mechanisms that enable proteins to carry out their biological functions. Among the several experimental approaches to the analysis of protein dynamics [for a review see Karplus and McCammon (1981)] is the measurement of polypeptide backbone amide hydrogen exchange rates. Linderstrøm-Lang (1955) and his colleagues (Hvidt & Linderstrøm-Lang, 1954; Linderstrøm-Lang & Schellman, 1959) first recognized that amide exchange rates are in some way determined by protein structural fluctuations. However, hydrogen exchange rates

are also sensitive to a variety of physical and chemical variables, and these must be specified before the contribution from molecular structure and/or motion in a protein can be deduced. To analyze these factors in the absence of contributions from secondary and tertiary protein structure, amide exchange has been studied in N-methylacetamide, small peptides, polymers of alternating D- and L-amino acids [for a review see Englander and Kallenbach (1984); Barksdale & Rosenberg, 1982)] and heat-unfolded BPTI[1] (Roder et al., 1985b). Numerous studies have shown that amide exchange is catalyzed by H_3O^+, OH^-, and, to a small extent, H_2O, according to

$$k_{ex} = k_{OH}[OH^-] + k_H[H_3O^+] + k_{H_2O} \qquad (1)$$

Often, hydrogen exchange is measured by using deuterium or tritium, and small kinetic and equilibrium isotope effects have been determined (Englander & Poulson, 1969; Barksdale & Rosenberg, 1982). Exchange rates increase about 3-fold for each 10 °C rise in temperature. (Englander et al., 1979; Gregory et al., 1983; Roder et al., 1985b). The inductive effects of neighboring side chains and peptide bonds were measured by Molday et al. (1972) for all 20 amino acids and for the amino and carboxyl termini of peptides. The results of these studies enable accurate predictions of amide exchange rates for simple aqueous systems if the pH, temperature, and amino acid sequence are specified. Less well calibrated are the effects of long-range electrostatic interactions and apolar environments. Kim and Baldwin (1982) studied the pH dependence of exchange in poly(D,L-lysine). They observed that, in the absence of salt, the pH_{min} for amide exchange in this polymer is about 2 pH units lower than that for the uncharged PDLA. They concluded that the pH near the surface of the PDLL molecule must be higher than that of the bulk solution due to the condensation of hydroxyl ions by the positive charges of the linear polymer. The effects of specific electrostatic interactions on the pH dependence of exchange in proteins were studied by Matthew and Richards (1983).

Leichtling and Klotz (1966) showed that dioxane, added to water, both retards exchange (i.e., lowers the rate of exchange, k_{min}, at the pH_{min}) and increases the pH_{min} by increasing pK_w. However, Perrin and Lollo (1984b) point out that this mixed-solvent model is not likely to apply to the apolar interior of a protein since the latter is in equilibrium with bulk water. They also conclude that a hydrophobic environment

will elevate the pH_{min} and depress k_{min}, not owing to any change in pK_w in the interior of the protein but because base-catalyzed exchange (k_{OH}) will be retarded more than acid-catalyzed exchange (k_H). This difference is the result of the high energy required for solvating the peptide amide transition state for the base-catalyzed mechanism, which contains a full negative charge, whereas for acid catalysis by the imidic acid mechanism the transition state is uncharged (Perrin & Lollo, 1984a,b; Perrin & Arrhenius, 1982). Interestingly, since primary amides ($CONH_2$) exchange via N-protonation (Perrin et al., 1980; Perrin & Johnston, 1981; Krishna et al., 1982), their acid-catalyzed transition states are positively charged, and k_{OH} and k_H are expected to be equally depressed in a hydrophobic environment. For primary amides, then, no shift in pH_{min} is expected, although the hydrophobic effect may depress k_{min}.

In water, buffer ions will not usually catalyze exchange because of their low pK_a's relative to the pK_a's of amides (Englander & Kallenbach, 1984). In a more nonpolar environment general acid–base catalysis by low concentrations of buffer ions may be significant. For example, Klotz and Frank (1965) measured a 10–15-fold rate enhancement for N-methylacetamide exchange in D_2O/dioxane due to only 76 mM imidazole.

Despite the intense efforts to characterize hydrogen exchange in unstructured peptides, the interpretation of protein hydrogen exchange data is controversial. Two different models have been proposed to account for the molecular motions in proteins that enable hydrogen bonds to break and hydrogen exchange to occur. In penetration models it is proposed that small-amplitude, high-frequency fluctuations open up channels in the protein to allow diffusion of catalysts (water) to amides that would otherwise be inaccessible (Woodward & Hilton, 1979; Karplus & McCammon, 1981; Matthew & Richards, 1983). The local unfolding models propose that cooperative unfolding of segments of secondary structure breaks the hydrogen bonds transiently, exposing the amide to solvent for exchange (Englander & Kallenbach, 1984; Karplus & McCammon, 1981; Roder et al., 1985a). One problem in distinguishing between the present models is that too few studies have been done in which individual amide proton exchange rates have been measured in proteins. However, recent developments in high-resolution NMR spectroscopy, including the use of two-dimensional spectroscopy (Wüthrich, 1986) as well as methods for improving the sensitivity of nuclei with low gyromagnetic ratios such as ^{15}N (Griffey et al., 1985; Griffey & Redfield, 1987), promise to overcome this deficiency and provide a more reliable data base on which to build models of protein amide exchange.

Recently, we have been investigating the hydrogen exchange properties of a small integral membrane protein (M13 coat protein) made soluble with the use of sodium dodecyl sulfate. These studies have included measurements of individual amide exchange rates for the most rapidly exchanging amides in the protein (Henry et al., 1987) as well as exchange rates for the most slowly exchanging amides that occur in the most hydrophobic segment of the sequence (O'Neil & Sykes, 1988). In order to determine the possible effects of the detergent micelle on the hydrogen exchange of the protein, we have measured the pH dependence of hydrogen exchange for an unstructured hydrophobic tripeptide dissolved with dodecyl sulfate micelles.

EXPERIMENTAL PROCEDURES

Materials. DSS and perdeuteriated sodium dodecyl sulfate were purchased from MSD Isotopes (Pointe Claire, Canada),

---

[1] Abbreviations: BPTI, basic pancreatic trypsin inhibitor; cmc, critical micelle concentration; COSY, homonuclear two-dimensional correlation spectroscopy; $\Delta H°_w$ enthalpy of autoionization of water; D_2O, deuterium oxide; DOC, deoxycholate; DSS, disodium 2,2-dimethyl-2-silapentane-5-sulfonate; DTAB, dodecyltrimethylammonium bromide; F, Faraday's constant; GCS, Gouy–Chapman–Stern; H_E, anti diastereotopic primary amide proton; H_Z, syn diastereotopic primary amide proton; $[H^+]_0$, proton concentration at a micelle surface; $[H^+]_\infty$, proton concentration in bulk solution; HPLC, high-performance liquid chromatography; I, ionic strength; k_D, acid-catalyzed exchange rate constant measured in D_2O; k_{ex}, measured amide hydrogen exchange rate; K_{D_2O}, equilibrium constant for the dissociation of D_2O; k_H, acid-catalyzed exchange rate constant measured in 85% H_2O/15% D_2O; k_{min}, minimum exchange rate in exchange versus pH profile; k_{OD}, base-catalyzed exchange rate constant measured in D_2O; k_{OH}, base-catalyzed exchange rate constant measured in 85% H_2O/15% D_2O; K_w, equilibrium constant for the dissociation of water; LiDS, lithium dodecyl sulfate; NMR, nuclear magnetic resonance; OG, octyl glucoside (n-octyl β-D-glucopyranoside); PDLL, poly(D,L-lysine); pH_{min}, pH corresponding to k_{min} in exchange versus pH profile measured in 85% H_2O/15% D_2O; pD_{min}, pD corresponding to k_{min} in exchange versus pD profile measured in D_2O; ppm, parts per million; PDLA, poly(D,L-alanine); pD, calculated deuterium ion activity in D_2O; pH*, pH meter reading in D_2O; R, universal gas constant; SDS-d_{25}, perdeuteriated sodium dodecyl sulfate; 12-DS, 12-doxylstearic acid; T_1, spin–lattice relaxation time; Y_0, electrostatic potential at a micelle surface.

and the perdeuteriated acetic acid and DCl were from Stohler Isotope Chemicals (Rutherford, NJ). D_2O was purchased from Bio-Rad Laboratories (Richmond, CA). The LiDS, DTAB, and OG were purchased from Sigma Chemical Co. (St. Louis, MO). The synthetic peptide Leu-Val-Ile-amide was provided by the Alberta Peptide Institute. Its purity was checked by amino acid analysis, ^1H NMR spectroscopy, and HPLC. Doxylstearic acid, labeled at carbon-12, was purchased from Molecular Probes (Junction City, OR).

Methods. Proton efflux from the peptide amides of Leu-Val-Ile-amide was initiated by dissolving the freeze-dried tripeptide sample in 0.5 mL of a buffered D_2O solution at 5 °C. The concentration of peptide was between 6.7 and 9.6 mM. Solutions also contained 100 mM LiCl and 30 mM phosphoric acid at high pD and 82 mM acetic acid-d_4 at lower pD. When detergent was present, it was 50 mM LiDS. LiDS was used since, unlike SDS, it is soluble at low temperatures. It may be noted that catalysis of hydrogen exchange by buffer ions is negligible due to their low pK_a's relative to the pK_a for the peptide bond amide (Englander & Kallenbach, 1984).

^1H NMR spectra, at 300 MHz, of freshly dissolved peptide in 5-mm NMR tubes were recorded with the use of a Nicolet NT 300 WB NMR spectrometer. The pulse width was 9 μs (90°), and the acquisition time was 1 s. The high concentration of detergent in some experiments created a dynamic range problem that was solved by saturation of the detergent methylene resonances at 1.30 ppm. The solvent signal was reduced by using a "jump and return" pulse sequence $(1,\bar{1})$ (Plateau & Gueron, 1982). Usually, 108 scans were required to achieve a reasonable signal-to-noise ratio in the amide region of the spectrum.

Hydrogen exchange rates were also determined by measuring the transfer of saturation by exchange from the H_2O resonance (Forsen & Hoffman, 1963, 1964; Gadian, 1982). For these measurements spectra were acquired with a Varian VXR500 NMR spectrometer at 25 °C in 85% H_2O/15% D_2O with preirradiation of the water resonance for 1.7 s. The pulse width was 14 μs (90°), and the acquisition time was 1 s. When the exchange rate (k_{ex}) between the labile amide and water is equal to or faster than the spin–lattice relaxation rate of the amide proton ($1/T_1$), the amide intensity will be reduced relative to its intensity in the absence of exchange by saturation transfer; it can be shown in general that

$$\text{fractional amide intensity} = 1/(1 + k_{ex}T_1) \qquad (2)$$

The standard inversion-recovery experiment was used to measure the T_1 values at the pH_{min} for the four different exchangeable amides in the peptide in their various environments. Thus, by measurement of the fractional amide intensity and the T_1 (in the absence of exchange), the exchange rate can be calculated. Additionally, since k_{ex} is pH dependent (eq 1), a pH titration of the amide intensity will yield k_{OH} and k_H and thus the pH_{min} for exchange (eq 5).

The detergent titration of the tripeptide was done at 24 °C by using perdeuteriated SDS, which did not obscure the tripeptide resonances. ^1H NMR spectra at 400 MHz were recorded with a Varian XL400 NMR spectrometer. The pulse width was 19 μs (90°), and the acquisition time was 1.5 s. The experiments with 12-doxylstearate were done on a Varian VXR500 NMR spectrometer. The pulse width was 12.5 μs (90°), and the acquisition time used was 2.5 s.

The deuterium ion activity in D_2O was corrected for the glass electrode reading error by using the equation from Glasoe and Long (1960):

$$pD = pH^* + 0.40 \qquad (3)$$

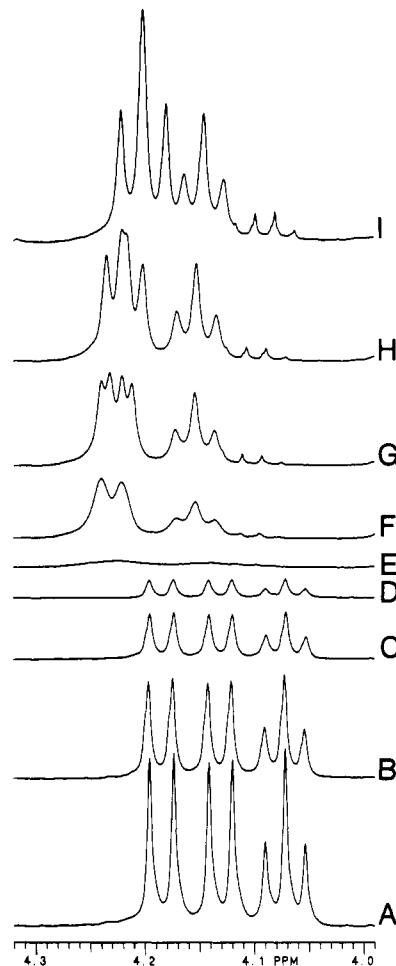FIGURE 1: αCH region of 400-MHz ^1H NMR spectra of the tripeptide Leu-Val-Ile-amide at various concentrations of SDS-d_{25}. The tripeptide concentration was 18.7 mM in D_2O, 115 mM acetic acid-d_4, pD 3.2, and 135 mM LiCl at 25 °C. SDS-d_{25} was added to obtain SDS-d_{25}/tripeptide molar ratios of (A) 0, (B) 0.1, (C) 0.3, (D) 0.6, (E) 1.3, (F) 3.2, (G) 4.8, (H) 7.02, and (I) 12.2. For each spectrum 1000 scans were averaged, and the spectra were processed with 0.5-Hz line broadening.

This correction is only approximate since the constant 0.40 was determined at 25 °C and the experiments in D_2O were done at 5 °C. Changes in the pH* of solutions containing Li^+ were made with dilute solutions of LiOH or DCl. Chemical shifts were measured relative to the methyl resonances of DSS.

RESULTS AND DISCUSSION

Interaction of the Tripeptide with SDS. The tripeptide Leu-Val-Ile-amide contains a single positive charge at its amino terminus that accounts for its solubility in water. Figure 1A shows the αCH region of a ^1H NMR spectrum of the peptide in D_2O. The upfield triplet in the spectrum (4.070 ppm) is easily assigned to the leucine αCH; downfield of the triplet are two doublets from the Val (4.130 ppm) and Ile αCH's (4.185 ppm). These resonances were assigned on the basis of a double-quantum filtered COSY experiment (data not shown). Despite its water solubility, the peptide also interacts with SDS in a specific fashion that depends upon the state of the detergent. When small amounts of SDS-d_{25} are added to a solution of the peptide, the ^1H NMR signals decrease progressively (Figure 1B–E) and a precipitate is observed in the NMR tube. Perdeuteriated SDS is used so that the detergent does not obscure the peptide resonances. Eventually, at about a 1:1 molar ratio of SDS-d_{25}/peptide, all of the peptide is precipitated from solution (Figure 1E). When
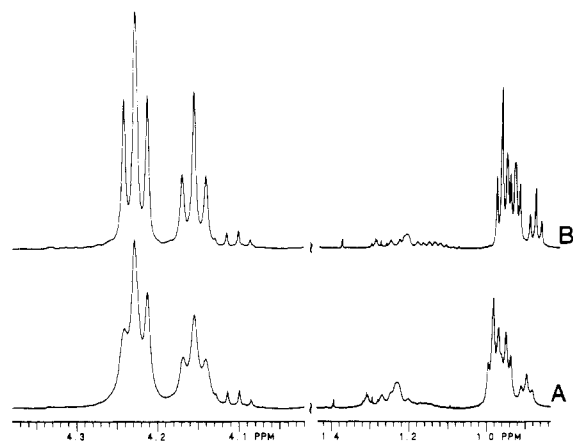
FIGURE 2: αCH region and aliphatic region of 500-MHz ^{1}H NMR spectra of the tripeptide Leu-Val-Ile-amide in SDS-d_{25} micelles in the absence (A) and presence (B) of 12-doxylstearic acid. The tripeptide was 4.6 mM in D$_2$O and 30 mM SDS-d_{25}, 50 mM phosphate, pD 7.4, and 100 mM LiCl at 30 °C; 0.1 mg of 12-doxylstearate was added to obtain a molar ratio of SDS-d_{25}/12-doxylstearate of about 2000:1. Each spectrum is the average of 1000 scans; the vertical scale of the αCH region is different from that of the methyl region. No line broadening of resolution enhancement was used in the processing of the spectra.

SDS-d_{25} is added to the precipitated peptide at a ratio that exceeds equimolar, the peptide goes back into solution and its ^{1}H NMR spectrum returns (Figure 1F–I), although the chemical shifts of the αCH resonances have changed significantly from what they were in the absence of detergent. At a SDS-d_{25}/peptide ratio of 12.2, for example, the triplet Leu αCH resonates at 4.145 ppm, and the Val and Ile doublets centered at 4.18 and 4.23 ppm, respectively, partially overlap. The nature of the small peaks upfield of the Leu triplet in spectra 1F–I is not certain.

At low SDS concentrations it is likely that the cationic peptide is interacting with anionic detergent monomers, which form a salt by virtue of their opposite charges. On the other hand, when SDS is present in excess of the peptide, the ionic interaction with detergent is supplemented by a hydrophobic interaction. Under the conditions of this experiment the critical micelle concentration of the detergent is approximately 1.3 mM (Mukerjee, 1967). However, the amount of SDS that must be added to reach the cmc is much higher than this since the SDS added is precipitated by the peptide; the effective cmc is the predicted cmc in the absence of peptide plus the concentration of the peptide. Solubilization of the peptide is therefore concomitant with the onset of micelle formation (see the legend to Figure 1).

To further explore the nature of the micelle/tripeptide interaction, a spin-labeled fatty acid was added to the mixture. The labeled fatty acid is water insoluble but is known to be taken up into SDS micelles (Waggoner et al., 1969). The addition of the spin label to SDS micelles broadens the ^{1}H NMR resonances of the detergent (not shown) because the spin label comes into close proximity with the hydrocarbon chain of the detergent [see also Waggoner et al. (1967)]. A similar result was obtained when spin-labeled stearate was added to the detergent-solubilized tripeptide. Figure 2A shows the αCH region and aliphatic region of a ^{1}H NMR spectrum of the tripeptide in SDS-d_{25}. When 12-DS was added to this sample, the spectrum with broadened resonances shown in Figure 2B was obtained. All three αCH resonances, the Ile-δ methyl triplet at 0.90 ppm, the overlapping Leu-δ and Val-γ methyl resonances at 0.92–1.01 ppm, and the Ile-γ methylene resonances at 1.23 ppm, are considerably broadened by the

spin label. However, the small peaks upfield of the Leu αCH triplet are not affected by the spin label, suggesting that they are not confined to the micelle. Not shown in the spectrum is the resonance line from formate ion that was added to the mixture. This small, negatively charged, polar molecule is apparently excluded from the SDS micelle, as its resonance line is unperturbed by the spin label on the fatty acid.

These experiments strongly suggest that the tripeptide preferentially associates with the detergent micelle. In view of the amphipathic nature of the tripeptide, two possible locations for the peptide suggest themselves: One possibility is that the peptide is inserted into the micelle with its positively charged amino terminus at the surface and the carboxyl-terminal amide buried in the interior of the micelle. This topology would maximize the hydrophobic and ionic interactions between the peptide and the detergent molecules but would do so at the expense of hydrogen bonds between the solvent and the amide backbone protons and carbonyl oxygens, which are unlikely in the micelle interior. Alternatively, the amphipathic peptide could be adsorbed onto the surface of the micelle that, in addition to being negatively charged, must also contain some hydrophobic patches (Tanford, 1973). At the surface the peptide could satisfy its ionic and hydrogen-bonding requirements as well as maintain some hydrophobic contacts with exposed detergent hydrocarbon. This simple analysis suggests that the latter topology will have a lower free energy than the former.

The experiments described above cannot distinguish between these two locations; however, a comparison to the building of molecules at membrane surfaces will illustrate the forces at work. Membranes are almost completely impermeable to small inorganic ions (Honig et al., 1986), but small ions will readily adsorb onto the surfaces of charged membranes (Winiski et al., 1986). Small amphipathic ions also adsorb onto membrane surfaces but will slowly migrate across a membrane bilayer; amphiphathic ions with long hydrocarbon chains also bind to membrane surfaces but show a stronger affinity for the membrane interior by their much more rapid transmembrane migration (Hartsel & Cafiso, 1986). These considerations suggest that the amphipathic tripeptide binds to the surface of the micelle and that the nonpolar parts of the peptide may occasionally penetrate the interior.

Kinetic Measurements of Amide Hydrogen Exchange. Hydrogen exchange rates were determined for the amide protons of Leu-Val-Ile-amide by using an exchange-out method in D$_2$O at 5 °C. Figure 3A shows the amide region of a ^{1}H NMR spectrum of the peptide 6.5 min after dissolution in a D$_2$O solution containing 50 mM LiDS at pD 5.8. The two singlet resonances at 7.00 and 7.53 ppm are the carboxyl-terminal (primary) amide protons. The Z (syn) substituent is always assigned to higher field and the E (anti) substituent to lower field (Perrin et al., 1980). The broad "doublet" at 7.99 ppm is the backbone amide proton of Ile. Spectra B–E show the decay of these resonances at increasing times after dissolution in D$_2$O. Not present in these spectra is the signal from the backbone amide proton of the Val residue, which exchanges too rapidly to be observed at pD 5.8. The Val amide doublet is observed at pD 3.8 and is shown in Figure 3F at 8.46 ppm. Conversely, at this low pD, the carboxyl-terminal amide protons exchange rapidly and escape detection. The assignment of the resonances was proved with a double-quantum filtered COSY spectrum of the peptide.

The exchange experiments shown in Figure 3 were repeated at several pD values in both the presence and absence of detergent. The amide resonance peak heights were measured

Table I: Summary of the Peptide Amide Exchange Rate Constants for Leu-Val-Ile-NH$_2$ Measured by Exchange-Out at 5 °C in D$_2$O and Dodecyl Sulfate[a]

		k_{OD} (M^{-1} s^{-1})	k_D (M^{-1} s^{-1})	k_{min} (s^{-1})	pD$_{min}$	ΔpD$_{min}$
CONH$_2$(Z)	D$_2$O	[8 × 10^7]	[30]	1.2 × 10^{-3}	4.7	
Ile–NH	D$_2$O	(6.0 ● 0.1) × 10^7	(1.2 ± 0.2) × 10^{-2}	2.5 × 10^{-5}	2.99	
Val–NH	D$_2$O	(4.0 ± 0.1) × 10^9	(8 ± 2) × 10^{-3}	2.0 × 10^{-4}	1.9	
CONH$_2$(Z)	LiDS	(2.1 ± 0.3) × 10^6	(4.3 ± 0.5) × 10^2	8.6 × 10^{-4}	6.0	1.3
Ile–NH	LiDS	(1.8 ± 0.4) × 10^6	1.2 ± 0.2	4.17 × 10^{-5}	4.76	1.77
Val–NH	LiDS	(2.00 ± 0.04) × 10^8	0.4 ± 0.1	3.2 × 10^{-4}	3.5	1.6

[a] The data in Figure 4 were fit to eq 4 in the text. k_{OD} and k_D are the first-order catalytic rate constants determined from the fits. The errors are the calculated standard deviations of the fits. The pD$_{min}$ and k_{min} values were calculated by using eq 5 and 6, respectively. ΔpD$_{min}$ = pD$_{min}$(LiDS) – pD$_{min}$(D$_2$O). D$_2$O designates experiments carried out in D$_2$O. LiDS designates experiments done in 50 mM LiDS in D$_2$O. The numbers in square brackets indicate the parameters used to draw lines to guide the eye through the CONH$_2$ data in Figure 4.
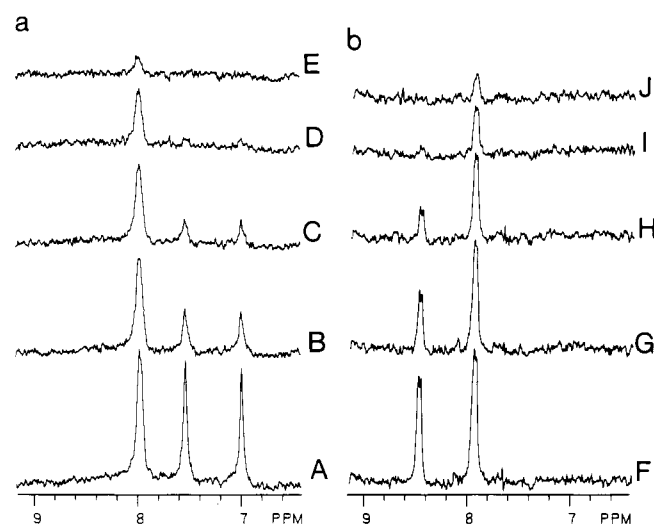

FIGURE 3: (a) Low-field region of 300-MHz ^{1}H NMR spectra showing the time courses of amide proton exchange for the tripeptide Leu-Val-Ile-amide in LiDS micelles: (A) 6.5, (B) 22, (C) 33, (D) 51, and (E) 121 min after dissolution in D$_2$O at pD 5.8 and 5 °C. The tripeptide was 7.4 mM in 50 mM LiDS, 100 mM LiCl, 82 mM acetic acid-d_4, and 25 mM phosphoric acid. The Ile amide proton resonates at 7.99 ppm, and the two carboxyl-terminal amides resonate at 7.00 and 7.53 ppm. (b) Time course of amide exchange at pD 3.8; the Val amide at 8.46 ppm is observed to exchange slowly. The Ile amide is observed at 7.92 ppm in spectra F–J. Conditions were as above except that tripeptide was 8.9 mM and phosphoric acid was absent. The exchange times are (F) 11.5, (G) 31, (H) 48, (I) 81, and (J) 134 min. All spectra were acquired with saturation of the LiDS methylene resonance and by using a jump-and-return pulse sequence (1.1) to reduce the solvent resonance. All spectra are the average of 108 scans and were processed with a 2-Hz line broadening.

and fit to exponential decays with a nonlinear, least-squares fitting routine. The pD dependence of the exchange rates determined from the fits is summarized in parts A and B of Figure 4 for exchange in the absence and presence of detergent, respectively. It was assumed that catalysis by D$_2$O is negligible, so that the lines through the points in these graphs are nonlinear least-sqares fits to equations of the form

$$k_{ex} = 10^{pD-pK_{D2O}}k_{OD} + 10^{-pD}k_D \qquad (4)$$

The pD$_{min}$ and k_{min} values (Table I) were calculated from the k_{OD} and k_D values by using the following equations from Leichtling and Klotz (1966):

$$pD_{min} = \tfrac{1}{2}pK_{D2O} - \tfrac{1}{2}\log(k_{OD}/k_D) \qquad (5)$$

$$k_{min} = 10^{-pD_{min}}2k_D \qquad (6)$$

The value for pK_{D2O} (=15.66) was calculated by using an equation from Roder et al. (1985b) based on experiments by Covington et al. (1966).

The values of k_{OD}, k_D, k_{min}, and pD$_{min}$ (Table I), determined for the amides of the tripeptide in the absence of detergent, are very similar to the published values for similar peptides
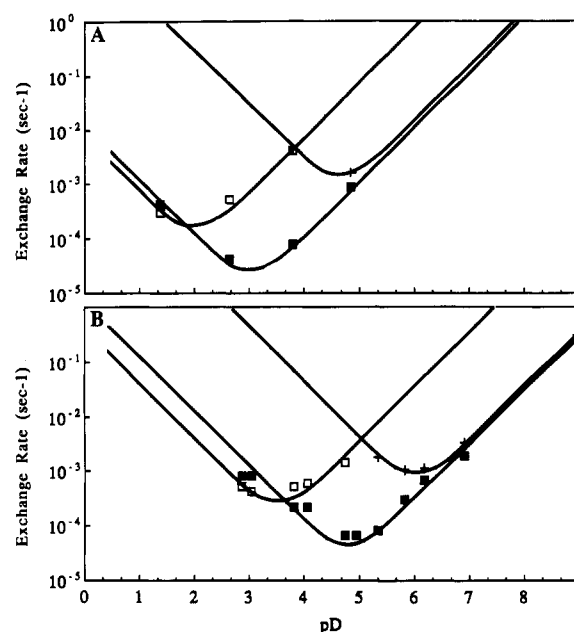
FIGURE 4: pD dependence of amide proton exchange in the tripeptide Leu-Val-Ile-amide in the absence (A) and presence (B) of LiDS micelles. Except for the lines through the Val–NH data in D$_2$O, the lines through the points are least-squares fits of the data to eq 3 given in the text. Not enough points were collected for a least-squares fit of the CONH$_2$ experiments in D$_2$O, and the lines through the points are meant to guide the eye. The main effect of the detergent is to increase the pD$_{min}$ of exchange for all of the measured amides: Ile–NH (■); Val–NH (□); carboxyl-terminal amides (+).

(Molday et al., 1972; Englander et al., 1972). The Val backbone amide has the lowest pD$_{min}$ (1.9), owing to the inductive effect of the positively charged amino terminus. The pD$_{min}$ (2.99) of the Ile backbone amide is very similar to that predicted for an amino acid located between two amino acids whose side chains have no measurable influence on hydrogen exchange (inductive effect = 0). The pD$_{min}$ of 4.7, measured for the carboxyl-terminal Z-amide, is similar to the pH*$_{min}$ of 4.4 measured for the Asn side-chain amide (Molday et al., 1972) and to the pH$_{min}$ of 4.31 measured for the Z-proton of N-acetyl-Gly-NH$_2$ (Krishna et al., 1982). Since amide exchange for small molecules in D$_2$O has been exhaustively studied, the purpose of these experiments was to confirm that the tripeptide exchange kinetics were in agreement with the literature. Nevertheless, because the Ile backbone amide exchanges slower than the other two, enough data were collected to accurately measure its exchange parameters independently of the literature values. The kinetic parameters measured for the Val amide and the terminal amide are less well determined but agree with the literature values.

Similar to the situation in D$_2$O, the Ile backbone amide proton exchanges slower in LiDS than the other three protons, and its kinetic parameters are therefore more accurately de-

Table II: Parameters from the Nonlinear Least-Squares Fits of the pH Dependence of Peptide Amide Proton Exchange in Leu-Val-Ile-NH$_2$ Determined by the Saturation-Transfer Method at 25 °C[a]

		T_1 (s)	k_{OH} (M^{-1} s^{-1})	k_H (M^{-1} s^{-1})	k_{min} (s^{-1})	pH$_{min}$	ΔpH$_{min}$	$\Delta \log k_{OH}$
CONH$_2$(Z)	H$_2$O	0.45	$(7.9 \pm 0.5) \times 10^7$	186 ± 13	2.4×10^{-2}	4.18		
CONH$_2$(E)	H$_2$O	0.40	$(1.2 \pm 0.7) \times 10^8$	113 ± 8	2.4×10^{-2}	3.98		
Ile-NH	H$_2$O	0.48	$(1.02 \pm 0.06) \times 10^8$					
Val-NH	H$_2$O	0.48	$(9.5 \pm 0.3) \times 10^9$					
CONH$_2$(Z)	SDS	0.58	$(4.9 \pm 0.7) \times 10^6$	$(2.7 \pm 0.4) \times 10^3$	2.4×10^{-2}	5.36	1.18	1.20
CONH$_2$(E)	SDS	0.58	$(4.2 \pm 0.6) \times 10^6$	$(1.6 \pm 0.2) \times 10^3$	1.7×10^{-2}	5.28	1.30	1.45
Ile-NH	SDS	0.59	$(3.1 \pm 0.4) \times 10^6$					1.52
Val-NH	SDS	0.58	$(1.52 \pm 0.06) \times 10^8$					1.80
CONH$_2$(Z)	SDS/salt	0.58	$(9.1 \pm 0.8) \times 10^6$	493 ± 47	1.4×10^{-2}	4.86	0.68	0.94
CONH$_2$(E)	SDS/salt	0.53	$(1.0 \pm 0.1) \times 10^7$	279 ± 38	1.0×10^{-2}	4.73	0.75	1.08
Ile-NH	SDS/salt	0.49	$(5.7 \pm 0.9) \times 10^6$					1.25
Val-NH	SDS/salt	0.50	$(1.9 \pm 0.1) \times 10^8$					1.70
CONH$_2$(Z)	DTAB	0.44	$(8.6 \pm 0.4) \times 10^7$	229 ± 10	2.8×10^{-2}	4.21	0.03	-0.04
CONH$_2$(E)	DTAB	0.40	$(1.2 \pm 0.1) \times 10^8$	147 ± 7	2.7×10^{-2}	4.04	0.06	0.0
Ile-NH	DTAB	0.49	$(1.00 \pm 0.04) \times 10^8$					0.01
Val-NH	DTAB	0.50	$(1.00 \pm 0.06) \times 10^{10}$					-0.02
CONH$_2$(Z)	OG	0.44	$(1.0 \pm 0.1) \times 10^8$	277 ± 23	3.4×10^{-2}	4.21	0.03	-0.10
CONH$_2$(E)	OG	0.40	$(1.3 \pm 0.1) \times 10^8$	192 ± 12	3.2×10^{-2}	4.08	0.10	-0.03
Ile-NH	OG	0.48	$(1.17 \pm 0.06) \times 10^8$					-0.06
Val-NH	OG	0.50	$(1.00 \pm 0.06) \times 10^{10}$					-0.02

[a] The data in Figure 5 were fit to eq 3 by using the measured T_1's (see text). k_{OH} and k_H are the first-order catalytic rate constants determined by the fits. The errors are the calculated standard deviations of the fits. The pH$_{min}$ values were calculated by using eq 5 in the text and the k_{OH} and k_H values. ΔpH$_{min}$ = pH$_{min}$(detergent) − pH$_{min}$(water). $\Delta \log [k_{OH}]$ = log $[k_{OH}]$(water) − log $[k_{OH}]$(detergent). H$_2$O designates experiments carried out in 85% H$_2$O/15% D$_2$O; SDS designates experiments carried out similarly but with the addition of 50 mM sodium dodecyl sulfate; SDS/salt designates experiments carried out in 0.6 M NaCl in addition to 52 mM sodium dodecyl sulfate. DTAB designates experiments carried out in 50 mM dodecyltrimethylammonium bromide; OG designates experiments in 50 mM octyl glucoside.

termined (Figure 4B, Table I). Because exchange rates greater than about 10^{-3} s^{-1} cannot be measured by using the direct exchange-out technique, measurements on the faster amides in detergent were restricted to pD values near the pD$_{min}$. Enough data were obtained for an accurate determination of the pD$_{min}$ and k_{min} in all cases, and this experiment shows that when the hydrophobic tripeptide is solubilized by a dodecyl sulfate micelle, a dramatic increase in the pD$_{min}$ for k_{ex} is observed for all of the exchangeable protons (Figure 4B; Table I). On the other hand, k_{min} is relatively unchanged by the detergent. The pD$_{min}$ increase was largest for the Ile backbone amide (1.77 units) and smallest for the Z-proton at the carboxyl terminus (1.3 units); k_{min} for the E-proton (data not shown) was slightly greater (1.1-fold) than for the Z-proton in both detergent and D$_2$O. The pD$_{min}$ increase for the Val amide was between these two values (1.6 units). A similar but opposite effect was observed by Kim and Baldwin (1982) for the pH dependence of k_{ex} in PDLL (see introduction). They explained their results using the counterion condensation theory for linear polyelectrolytes in solution (Manning, 1978). The negative electrostatic potential at the surface of an SDS micelle will also condense cations onto its surface, effectively lowering the pD there; this would result in the measurement of pD$_{min}$ for exchange that are higher than normal. The elevation of the pD$_{min}$ in the absence of any discernible change in k_{min} means that k_{OH} is depressed to the same extent as k_H is enhanced. This is readily accounted for if the only effect of the detergent is to alter the pD in the environment of the peptide, as the elevation in [D$^+$] must necessarily be equal to the decrease in [OD$^-$].

Since the peptide is in a low dielectric environment in LiDS (or at least at an interface between a high and a low dieletric) and also in a region of a high concentration of negatively charged oxygens (SO$_4^-$), it is perhaps surprising that no general base catalysis by the detergent is observed. As Table I shows, k_{OD} is depressed, not enhanced, as it would be if SO$_4^-$ catalysis of exchange was effective.

Another possible explanation for the elevated pD$_{min}$ would require a specific, hydrogen-bonding interaction between the peptide and the detergent. If the tripeptide is adsorbed onto the surface of the micelle, it is possible that the amide hydrogens form hydrogen bonds to the negatively charged oxygens on the detergent molecules. Since the base-catalyzed mechanism involves abstraction of a deuteron by OD$^-$ and a negatively charged transition state, the negative charge on the detergent would be expected to suppress the base-catalyzed reaction. The acid-catalyzed reaction of backbone amides would be enhanced by such an interaction but perhaps to a smaller extent than the base-catalyzed reaction would be suppressed because the transition state for the imidic acid mechanism is neutral (Perrin & Lollo, 1984a,b; Perrin & Arrhenius, 1982). For this effect we expect to observe a reduction of k_{min} in addition to an elevation of pD$_{min}$, whereas our observation is of a change only in pD$_{min}$.

Steady-State Measurements of Hydrogen Exchange. At pH's away from the pH$_{min}$, amide exchange in small unstructed peptides is too rapid to be measured kinetically even at 5 °C. In order to measure exchange in the alkaline and acid limbs of the exchange curves, we have used a steady-state technique based on saturation transfer (see Methods). Figure 5A shows the pH dependence of amide intensity in the NMR spectrum at 25 °C for the carboxyl-terminal amide Z-proton of the tripeptide. For the peptide in SDS both limbs of the titration curve are shifted to alkaline pH by about 1.2 units compared to the curve in water. Thus, acid catalysis is enhanced to the same extent as base catalysis is depressed. Enough data were acquired in both limbs of the titration curves for an accurate calculation of the pH$_{min}$, using eq 5 and the k_H and k_{OH} values from the least-squares fits of the data, and these are listed in Table II. The increase in pH$_{min}$ measured by saturation transfer at 25 °C (Table II) (ΔpH$_{min}$ = 1.20) is similar to the increase in pD$_{min}$ measured kinetically at 5 °C (Table I) (ΔpD$_{min}$ = 1.3). This agreement suggests that the same mechanism which raises the pD$_{min}$ at 5 °C for all the amides
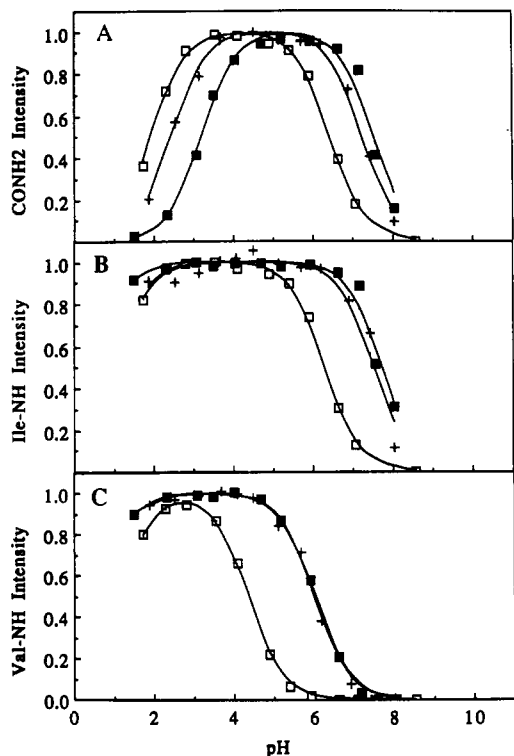
FIGURE 5: pH dependence of amide proton intensity due to saturation transfer for (A) the primary amide protons at the carboxyl terminus, (B) the secondary backbone amide proton of isoleucine, and (C) the secondary backbone amide proton of valine in the tripeptide Leu-Val-Ile-NH$_2$ in H$_2$O ($\square$), with the addition of 52 mM SDS-d_{25} ($\blacksquare$), and with the addition of 50 mM SDS-d_{25} plus 0.6 M NaCl (+). The pH titrations were carried out at 25 °C in 85% H$_2$O/15% D$_2$O, 9 mM Na$_2$HPO$_4$, 8 mM Na$_2$B$_4$O$_7$, 9 mM acetic acid-d_4, and 2.4 mM peptide. ^{1}H NMR spectra were acquired at 500 MHz with presaturation of the water resonance. The solid lines through the points are nonlinear least-squares fits of the data as described in the text using eq 3 and 4 and the values for T_1 given in Table II.

also explains the increased pH$_{min}$ for the primary (terminal) amides at 25 °C.

The acid-catalyzed rate constants (k_H) measured at 25 °C (Table II) for the primary amide in both SDS and H$_2$O are about 6-fold greater than those (k_D) measured at 5 °C (Table I). Because of the 20 °C difference in temperature between the two experiments, about a 9-fold difference in rates is expected (Englander & Kallenbach, 1984). The base-catalyzed rate constants (k_{OH}) at 25 °C, however, are similar to those (k_{OD}) measured at 5 °C. This is because the temperature dependence of the base-catalyzed reaction is dominated by the enthalpy of autoionization of water ($\Delta H°_w = 13.52$ kcal/mol). Thus, k_{OH} and k_{OD} values appear largely insensitive to temperature because of the use of temperature-sensitive pK_w and pK_{D_2O} values in eq 4. The pD$_{min}$ for the primary Z-amide measured in D$_2$O at 5 °C (Table I) is higher than that measured in H$_2$O at 25 °C (Table II) because when pH = pD, [OH$^-$] > [OD$^-$] due to the difference between pK_w and pK_{D_2O}. In other words, since pK_{D_2O} > pK_w, then pD$_{min}$ should be greater than pH$_{min}$ if $k_{OH}/k_H = k_{OD}/k_D$ in eq 5. The k_{min} measured at 25 °C (Table II) is about 20-fold greater in water and about 28-fold greater in detergent than those measured at 5 °C (Table I). From eq 6 it is clear that this is due to the difference between k_H and k_D and between pH$_{min}$ and pD$_{min}$ as discussed.

Table II also compares the rates of exchange for the two terminal amides. Generally, base-catalyzed exchange of H$_E$ is faster than exchange for H$_Z$, owing to the different acidities of the two protons (Perrin et al., 1981). Table II also shows

that the acid-catalyzed exchange of H$_Z$ is apparently faster than the exchange of H$_E$, whereas others have shown that H$_E$ and H$_Z$ exchange at about the same rate at low pH (Krishna et al., 1982; Perrin et al., 1980). This result was checked by measuring the T_1 and relative amide intensities of the two protons in water at pH 6.3 and 1.9. From these measurements values of $k_{ex}^E/k_{ex}^Z = 1.22$ at pH 6.3 and 0.62 at pH 1.9 were calculated. The relative rates of exchange of H$_E$ and H$_Z$ have been shown to be sensitive to inductive as well as solvent effects (Perrin et al., 1981). Also, the downfield NH's have been observed to exchange faster in the Gln and glycinamide residues in oxytocin (Krishna et al., 1979).

The pH dependence of the Ile and Val amide intensities at 25 °C are shown in parts B and C of Figure 5, respectively. Because the pH$_{min}$ for these amides are lower than for the C-terminal amides, relatively little data were measured in the acidic limbs of the titration curves. However, the k_{OH} values derived from the basic limbs for the Ile and Val amides in H$_2$O and in SDS at 25 °C are all in good agreement with the k_{OD} values measured at 5 °C in D$_2$O; each k_{OH} (Table II) is similar to its corresponding k_{OD} (Table I). The effect of SDS on the backbone amide exchange can be measured by the difference in k_{OH} measured in water and SDS ($\Delta \log k_{OH}$ in Table II) and these values are relatively close to the ΔpD$_{min}$ values shown in Table I and measured at 5 °C. Here, the effect of SDS is to decrease k_{OH}, presumably for the same reason that the pD$_{min}$ are elevated by LiDS at 5 °C.

To test whether the elevated pH$_{min}$ in SDS are due to an electrostatic effect (Kim & Baldwin, 1982), exchange was measured in high salt. Figure 5 shows the effect of 0.6 M NaCl on the saturation-transfer-dependent amide intensities in Leu-Val-Ile-NH$_2$. Small shifts in the titration curves resulted from the presence of high salt, and small shifts in pH$_{min}$ and $\Delta \log k_{OH}$ ranging from 0.1 to 0.5 pH unit were calculated (Table II). Unfortunately, because of broader line widths and higher noise in the spectra, the titrations in high salt are less accurate than the experiments done in low salt, and the scatter in the titration curves makes conclusions based on them less reliable. Nevertheless, it is clear that salt has a small but measurable effect on all of the measured pH$_{min}$ and k_{OH}.

Amide exchange rates for Leu-Val-Ile-amide were also measured in the presence of a neutral detergent, octyl glucoside, and a positively charged detergent, dodecyltrimethylammonium bromide. Table II shows that these detergents had little or no effect on the exchange kinetics of the peptide amides, as most of the kinetic parameters are quite close to the values measured in water. Addition of 12-DS to solutions of peptide and these detergents had almost no effect on the ^{1}H NMR spectrum of the peptide, whereas the detergent resonances were considerably broadened. This suggests that the positively charged peptide does not associate with either the positive or neutral detergent.

If the measured ΔpD$_{min}$, ΔpH$_{min}$, and $\Delta \log k_{OH}$ are due to an electrostatically generated difference between [H$^+$]$_0$ at the surface of an SDS micelle and [H$^+$]$_\infty$ in bulk solution, then it should be possible to calculate the pH at the surface as well as the change in pH at the surface due to changing the ionic strength of the solution by using the relation

$$[H^+]_0 = [H^+]_\infty \exp\left[\frac{F\psi_0{}^I}{RT}\right] \qquad (7)$$

where F is Faraday's constant, R is the gas constant, T is the absolute temperature, and $\psi_0{}^I$ is the electrostatic potential at the surface of the micelle at ionic strength I (Castle & Hubbell, 1976; Winiski et al., 1986). Values of $\psi_2{}^I$ (2.0 Å from

O'Neil and Sykes

the surface of the micelle) were calculated by Emerson and Holtzer (1965, 1967) from numerical solutions to the non-linearized Poisson–Boltzmann equation assuming that the micelle is a sphere with smeared charge. Using the known variations of micelle radius and micelle number with ionic strength, they calculated $\psi_2^{0.1} = 128$ mV and $\psi_2^{0.5} = 100$ mV. From eq 7 the difference in pH between bulk solution and the surface of the micelle at 0.1 M ionic strength will equal log $[\exp(0.128F/RT)] = 2.2$, which is somewhat larger than the ΔpD_{min} in Table I and the ΔpH_{min} and $\Delta \log k_{OH}$ in Table II. Also, addition of 0.4 M NaCl should change the $[H^+]_0$ at the surface of the micelle by $\exp[(F/RT)(0.128 - 0.100)] = 3$-fold or by about 0.5 pH unit; this is somewhat larger than the values calculated from Table II.

The discrepancy between the measured and calculated ΔpH_{min} might be due to the inadequacy of the model of a micelle including the assumption that the charge is smeared out over the surface. Although the charge on lipid bilayers and vesicles and detergent micelles is discrete, the electrostatic potential is often described theoretically by assuming the charge is smeared out uniformly over the surface (Gouy–Chapman–Stern theory). This theory was tested by Winiski et al. (1986), who measured the adsorption of a fluorescent, amphipathic anion and paramagnetic Mn^{2+} to charged bilayers, and by Hartsel and Cafiso (1986), who measured the binding of paramagnetic, cationic amphiphiles to charged lipid vesicles. Both of these studies showed that the binding of the ions and the electrostatic potential at the surfaces are well described by GCS theory. The theory is somewhat less successful in predicting the ΔpH_{min} for exchange in each of the amides in Leu-Val-Ile-amide due to SDS and its variation with ionic strength, which suggests that hydrogen exchange rates are not simply related to the average potential at the surface of the micelle, i.e., that discrete charge effects are important in determining the pH near an exchanging amide. It is possible that the peptide could significantly alter the ψ_0^I in its vicinity, changing both the pH at the surface and its dependence on ionic strength. Other problems in the calculation of ψ_0^I include the fact that micelles are elliptical in shape, becoming more asymmetric as the ionic strength increases, and that in solution a range of micelle shapes and sizes exist in equilibrium (Tanford, 1973).

CONCLUSIONS

In studies of amide exchange in the tripeptide Leu-Val-Ile-amide, dodecyl sulfate increases the pH_{min} for exchange of the primary and secondary amides by an electrostatic effect. In general, then, amide exchange rates measured for proteins dissolved in SDS should be compared to the rates of exchange of model compounds in the detergent, especially if the full pH dependence of exchange is not measured for the protein. Since a 2-pH-unit increase in the pH_{min} translates into a 100-fold retardation of exchange in the alkaline limb of the exchange curve (Figure 4), slowing factors will be seriously overestimated in the protein if the pH_{min} shifts are not taken into account. Knowledge of the exchange properties of the unstructured peptides in detergent has allowed us to separate the retardation of exchange due to protein structure in M13 coat protein dissolved in detergent from the apparent retardation due to a SDS-induced shift in the pH_{min} (O'Neil & Sykes, 1988).

REFERENCES

Barksdale, A. D., & Rosenberg, A. (1982) *Methods Biochem. Anal. 28,* 1–116.

Castle, J. D., & Hubbell, W. L. (1976) *Biochemistry 15,* 4818–4831.

Covington, A. K., Robinson, R. A., & Bates, R. G. (1966) *J. Phys. Chem. 70,* 3820–3824.

Emerson, M. F., & Holtzer, A. (1965) *J. Phys. Chem. 69,* 3718–3721.

Emerson, M. F., & Holtzer, A. (1967) *J. Phys. Chem. 71,* 1898–1907.

Englander, J. J., Calhoun, D. B., & Englander, S. W. (1979) *Anal. Biochem. 92,* 517–524.

Englander, S. W., & Poulson, A. (1969) *Biopolymers 7,* 379–393.

Englander, S. W., & Kallenbach, N. R. (1984) *Q. Rev. Biophys. 16,* 521–655.

Englander, S. W., Downer, N. W., & Teitelbaum, H. (1972) *Annu. Rev. Biochem. 41,* 903–924.

Forsen, S., & Hoffman, R. A. (1963) *J. Chem. Phys. 39,* 2892–2901.

Forsen, S., & Hoffman, R. A. (1964) *J. Chem. Phys. 40,* 1189–1196.

Gadian, D. G. (1982) *NMR and Its Applications to Living Systems,* pp 131–132, Clarendon, Oxford, U.K.

Glasoe, P., & Long, F. (1960) *J. Phys. Chem. 64,* 188–190.

Gregory, R. B., Crabo, L., Percy, A. J., & Rosenberg, A. (1983) *Biochemistry 22,* 910–917.

Griffey, R. H., & Redfield, A. G. (1987) *Q. Rev. Biophys. 19,* 57–82.

Griffey, R. H., Redfield, A. G., Loomis, R. E., & Dahlquist, F. W. (1985) *Biochemistry 24,* 817–882.

Hartsel, S. C., & Cafiso, D. S. (1986) *Biochemistry 25,* 8214–8219.

Henry, G. D., Weiner, J. H., & Sykes, B. D., (1987) *Biochemistry 26,* 3626–3634.

Honig, B. H., Hubbell, W. L., & Flewlling, R. F. (1986) *Annu. Rev. Biophys. Biophys. Chem. 15,* 163–193.

Hvidt, A., & Linderstrøm-Lang, K. (1954) *Biochim. Biophys. Acta 14,* 574–576.

Karplus, M., & McCammon, J. A. (1981) *CRC Crit. Rev. Biochem. 9,* 293–349.

Kim, P. S., & Baldwin, R. L. (1982) *Biochemistry 21,* 1–5.

Klotz, I. M., & Frank, B. H. (1965) *J. Am. Chem. Soc. 87,* 2721–2728.

Krishna, N. R., Huang, D.-H., Glickson, J. D., Rowan, R., & Walter, R. (1979) *Biophys. J. 26,* 345–366.

Krishna, N. R., Sarathy, K. P., Huang, D.-H., Stephens, R. L., Glickson, J. D., Smith, C. V., & Walter, R. (1982) *J. Am. Chem. Soc. 104,* 5051–5053.

Leichtling, B. H., & Klotz, I. M. (1966) *Biochemistry 5,* 4026–4037.

Linderstrøm-Lang, K. U. (1955) *Spec. Publ.–Chem. Soc. 2,* 1–20.

Linderstrøm-Lang, K. U., & Schellman, J. A. (1959) *Enzymes, 2nd, Ed. 1,* 443–510.

Manning, G. S. (1978) *Q. Rev. Biophys. 11,* 179–246.

Matthew, J. B., & Richards, F. M. (1983) *J. Biol. Chem. 258,* 3039–3044.

Molday, R. S., Englander, S. W., & Kallen, R. G. (1972) *Biochemistry 11,* 150–158.

Mukerjee, P. (1967) *Adv. Colloid Interface Sci. 1,* 241–267.

O'Neil, J. D. J., & Sykes, B. D. (1988) *Biochemistry 27*, 2753–2762.

Perrin, C. L., & Johnston, E. R. (1981) *J. Am. Chem. Soc. 103*, 4697–4703.

Perrin, C. L., & Arrhenius, G. M. L. (1982) *J. Am. Chem. Soc. 104*, 6693–6696.

Perrin, C. L., & Lollo, C. P. (1984a) *J. Am. Chem. Soc. 106*, 2749–2753.

Perrin, C. L., & Lollo, C. P. (1984b) *J. Am. Chem. Soc. 106*, 2754–2757.

Perrin, C. L., Johnston, E. R., & Ramirez, J. L. (1980) *J. Am. Chem. Soc. 102*, 6299–6304.

Plateau, P., & Gueron, M. (1982) *J. Am. Chem. Soc. 104*, 7310–7311.

Roder, H., Wagner, G., & Wüthrich, K. (1985a) *Biochemistry 24*, 7396–7407.

Roder, H., Wagner, G., & Wüthrich, K. (1985b) *Biochemistry 24*, 7407–7411.

Tanford, C. (1973) *The Hydrophobic Effect: Formation of Micelles and Biological Membranes*, Wiley, New York.

Waggoner, A. S., Griffith, O. H., & Christensen, C. R. (1967) *Proc. Natl. Acad. Sci. U.S.A. 57*, 1198–1205.

Waggoner, A. S., Kingzett, T. J., Rottschaefer, S., Griffith, O. H., & Keith, A. D. (1969) *Chem. Phys. Lipids 3*, 245–253.

Winiski, A. P., McLaughlin, A. C., McDaniel, R. V., Eisenberg, M., & McLaughlin, S. (1986) *Biochemistry 25*, 8206–8214.

Woodward, C. K., & Hilton, B. D. (1979) *Annu. Rev. Biophys. Bioeng. 8*, 99–127.

Wüthrich, K. (1986) *NMR of Proteins and Nucleic Acids*, Wiley, New York.

Photoaffinity Labeling of Terminal Deoxynucleotidyl Transferase. 1. Active Site Directed Interactions with 8-Azido-2'-deoxyadenosine 5'-Triphosphate[†]

Robert K. Evans and Mary Sue Coleman*

Department of Biochemistry and Lucille P. Markey Cancer Center, University of Kentucky Medical Center, Lexington, Kentucky 40536-0084

Received June 13, 1988; Revised Manuscript Received August 23, 1988

ABSTRACT: A photoaffinity analogue of dATP, 8-azido-2'-deoxyadenosine 5'-triphosphate (8-azido-dATP), was used to probe the nucleotide binding site of the non-template-directed DNA polymerase terminal deoxynucleotidyl transferase (EC 2.7.7.31). The Mg^{2+} form of 8-azido-dATP was shown to be an efficient enzyme substrate with a K_m of 53 μM. Loss of enzyme activity occurred during UV photolysis only in the presence of 8-azido-dATP. At saturation (120 μM 8-azido-dATP), 54% of the protein molecules were modified as determined by inhibition of enzyme activity. Kinetic analysis of enzyme inhibition induced by photoincorporation of 8-azido-dATP indicated an apparent K_d of ~38 μM. Addition of 2 mM dATP to 120 μM 8-azido-dATP resulted in greater than 90% protection from photoinduced loss of enzyme activity. In contrast, no protection was observed with the addition of 2 mM dAMP. Enzyme inactivation was directly correlated with incorporation of radiolabeled 8-azido-dATP into the protein and UV-induced destruction of the azido group. Photoincorporation of 8-azido-dATP into terminal transferase was reduced by all purine and pyrimidine deoxynucleoside triphosphates of which dGTP was the most effective. The α and β polypeptides of calf terminal transferase were specifically photolabeled by $[\gamma\text{-}^{32}P]$-8-azido-dATP, and both polypeptides were equally protected by all four deoxynucleoside triphosphates. This suggests that the nucleotide binding domain involves components from both polypeptides.

Terminal deoxynucleotidyl transferase (deoxynucleoside triphosphate:oligodeoxynucleotide deoxynucleotidyl transferase, EC 2.7.7.31) (terminal transferase)[1] is a DNA-polymerizing enzyme independent of DNA templates. Terminal transferase catalyzes a linear condensation polymerization reaction in vitro. Like all known DNA polymerases, terminal transferase requires an acceptor 3'-OH group (Kato et al., 1967) and metal chelate forms of (deoxy)nucleoside triphosphates. Unlike other polymerases, terminal transferase has a specialized tissue localization in prelymphocytes of mammalian bone marrow and thymus and in their differentiation-arrested counterparts (Coleman et al., 1974; Chang, 1971; McCaffrey et al., 1973). The expression of terminal transferase is correlated with the insertion of extra random nucleotides between the V, D, and J regions that accompany the rearrangement of immunoglobulin heavy chain genes or T cell receptor β genes during lymphoid ontogeny (Alt et al., 1982; Desiderio et al., 1984). Terminal transferase is synthesized as a catalytically active single polypeptide (60 kDa); however, lower M_r forms can be detected in crude tissue extracts and during enzyme purification (Chang et al., 1982; Deibel et al., 1983). These other two catalytically active enzyme forms result from specific

[1] Abbreviations: terminal transferase, terminal deoxynucleotidyl transferase; 8-azido-dATP, 8-azido-2'-deoxyadenosine 5'-triphosphate; Bis-Tris, [bis(2-hydroxyethyl)amino]tris(hydroxymethyl)methane; SDS, sodium dodecyl sulfate; BBOT, 2,5-bis(5-*tert*-butylbenzoxazo-2-yl)-thiophene.